

# Meson mass at real and imaginary chemical potentials

Kouji Kashiwa,<sup>1,\*</sup> Masayuki Matsuzaki,<sup>2,†</sup> Hiroaki Kouno,<sup>3,‡</sup> Yuji Sakai,<sup>1,§</sup> and Masanobu Yahiro<sup>1,¶</sup>

<sup>1</sup>*Department of Physics, Graduate School of Sciences, Kyushu University, Fukuoka 812-8581, Japan*

<sup>2</sup>*Department of Physics, Fukuoka University of Education, Munakata, Fukuoka 811-4192, Japan*

<sup>3</sup>*Department of Physics, Saga University, Saga 840-8502, Japan*

(Dated: August 28, 2018)

Chemical-potential dependence of pi and sigma meson masses is analyzed at both real and imaginary chemical potentials,  $\mu_R$  and  $\mu_I$ , by using the Polyakov-loop extended Nambu–Jona-Lasinio (PNJL) model that possesses both the extended  $\mathbb{Z}_3$  symmetry and chiral symmetry. In the  $\mu_I$  region, the meson masses have the Roberge-Weiss periodicity. The  $\mu_I$  dependence of the meson masses becomes stronger as temperature increases. We argue that meson masses and physical quantities in the  $\mu_R$  region will be determined from lattice QCD data on meson masses in the  $\mu_I$  region by using the PNJL model, if the data are measured in the future.

PACS numbers: 11.30.Rd, 12.40.-y, 21.65.Qr, 25.75.Nq

## I. INTRODUCTION

Extensive studies for exploring the phase diagram of Quantum Chromodynamics (QCD) have been done at finite temperature ( $T$ ) and chemical potential ( $\mu$ ). In the study of the quark-gluon system, lattice QCD (LQCD) is a powerful method if  $\mu = 0$ . LQCD, however, has the well known sign problem when the real part of  $\mu$  is finite; for example, see Ref. [1] and references therein. Therefore, several approaches such as the reweighting method [2], the Taylor expansion method [3], the analytic continuation from imaginary chemical potential  $\mu_I$  to real one  $\mu_R$  [4, 5, 6] and so on are suggested to circumvent the difficulty, but those are still far from perfection.

Constructing the effective model is an approach complementary to the first-principle LQCD simulation. For example, the phase structure and light meson masses at finite  $T$  and  $\mu_R$  are extensively investigated by the Nambu–Jona-Lasinio (NJL) model [7, 8, 9, 10, 11] and the Polyakov-loop extended Nambu–Jona-Lasinio (PNJL) model [12, 13, 14, 15, 16, 17, 18, 19, 20, 21, 22, 23, 24, 25, 26, 27, 28, 29, 30]. The NJL model can treat the chiral symmetry breaking, but does not possess the confinement mechanism. Meanwhile, the PNJL model is designed [14] to treat the confinement mechanism approximately in addition to the symmetry breaking. In this sense, the PNJL model is superior to the NJL model.

In the PNJL model with two flavor quarks, the model parameters are usually determined from the pion mass and the pion decay constant at  $T = \mu = 0$  and LQCD data at finite  $T$  and zero  $\mu$ ; see Sec. II for the details. However, the strength of the vector-type four-point interaction can not be determined at zero  $\mu$  and then remains as a free parameter, although the location of the critical endpoint of the chiral phase transition in the  $\mu_R$  region is found to be sensitive to the strength [11, 28, 31]. Thus, it is highly nontrivial how large the strength of the

vector-type interaction is and whether the PNJL model well simulates the  $\mu$  dependence of the phase structure and light meson masses. This should be tested directly from QCD. Fortunately, this is possible in the  $\mu_I$  region, since LQCD is feasible there because of the absence of the sign problem. Furthermore, it is possible to determine the strength of the interaction, for example the vector-type four quark and the higher-order multi-quark interaction, from LQCD data in the  $\mu_I$  region, as proposed by our previous paper [32].

In addition, the canonical partition function  $Z_C(n)$  with real quark number  $n$  can be obtained as the Fourier transform of the grand-canonical one  $Z_{GC}(\theta)$  with  $\mu = i\mu_I = i\theta T$  [33]:

$$Z_C(n) = \frac{1}{2\pi} \int_{-\pi}^{\pi} d\theta e^{-in\theta} Z_{GC}(\theta). \quad (1)$$

Thus, the thermodynamic potential,  $\Omega_{\text{QCD}}(\theta) = -T \ln(Z_{GC}(\theta))$ , at finite  $\theta$  contains the QCD dynamics at real  $n$  and hence at finite  $\mu_R$  in principle. Therefore, we can confirm the reliability of the PNJL model in the  $\mu_R$  region by comparing the model results with LQCD ones in the  $\mu_I$  region.

Roberge and Weiss (RW) found that  $\Omega_{\text{QCD}}(\theta)$  has a periodicity,  $\Omega_{\text{QCD}}(\theta) = \Omega_{\text{QCD}}(\theta + 2\pi k/3)$ , in the  $\mu_I$  region [33], where  $k$  is any integer. The RW periodicity indicates that QCD is invariant under the extended  $\mathbb{Z}_3$  transformation, that is, the combination of the  $\mathbb{Z}_3$  transformation and the coordinate transformation  $\theta \rightarrow \theta + 2\pi/3$ , as shown later in Sec. II; see our previous works [32] for the details. At the present stage the PNJL model is only a realistic model that possesses both the extended  $\mathbb{Z}_3$  symmetry and chiral symmetry. The PNJL model results are then consistent with LQCD ones particularly in the  $\theta$ -dependence of the Polyakov loop, the quark number density and the chiral condensate [32]. In the PNJL model, we do not need any extrapolation from the  $\mu_I$  to the  $\mu_R$  region, since the model calculation is feasible at finite  $\mu_R$  with the input parameters determined so as to reproduce LQCD data in the  $\mu_I$  region. We call this procedure the imaginary chemical-potential matching approach (the  $\theta$ -matching approach) in this paper.

In this paper, using the PNJL model, we predict the  $\mu$  dependence of pi and sigma meson masses in the real and imaginary  $\mu$  regions, and argue that meson masses and physical

\*kashiwa@phys.kyushu-u.ac.jp

†matsuzaki@fukuoka-edu.ac.jp

‡kounoh@cc.saga-u.ac.jp

§sakai@phys.kyushu-u.ac.jp

¶yahiro@phys.kyushu-u.ac.jp

quantities in the  $\mu_R$  region will be determined from LQCD data on meson masses in the  $\mu_I$  region by using the PNJL model, if the data are measured in the future. Concretely, the following four points are argued. First, we show that the meson masses have the RW periodicity. Second, the  $\theta$  dependence of meson masses is found to become large as  $T$  increases. We then recommend that LQCD simulations on meson masses in the  $\mu_I$  region be made at higher  $T$  near the pseudo-critical temperature  $T_c$  of the deconfinement phase transition at  $\mu = 0$ . Third, the validity of two extrapolations from  $\mu = \mu_I$  to  $\mu = \mu_R$  is discussed by comparing results of the extrapolations with the PNJL one. In recent LQCD calculations at finite  $\theta$ , only small lattice sizes are taken, so that pion mass evaluated in Ref. [34] is unnaturally large. This indicates that the bare quark mass ( $m_0$ ) taken there is rather large. Finally, we discuss how sensitive meson masses are to the value of  $m_0$ , comparing two cases of  $m_0 = 5.5$  and 80 MeV. This sort of model prediction is important before doing heavy LQCD calculations with large lattice size in the  $\mu_I$  region.

We briefly explain the PNJL model in section II and present equations for meson masses in section III. In section IV, numerical results are shown on the  $\mu$ -dependence of pi and sigma meson masses, and the validity of two extrapolation methods is discussed. Section V is devoted to summary.

## II. PNJL MODEL

In this section, we briefly review the PNJL model; see [32] for the details. The Lagrangian density of the two-flavor PNJL model is

$$\mathcal{L}_{\text{PNJL}} = \bar{q}(i\gamma_\nu D^\nu - m_0)q + G_s[(\bar{q}q)^2 + (\bar{q}i\gamma_5\vec{\tau}q)^2] - \mathcal{U}(\Phi[A], \bar{\Phi}[A], T), \quad (2)$$

where  $D^\nu = \partial^\nu + iA^\nu$ ,  $q$  denotes the quark field with two flavor and the current quark mass  $m_0$ . The field  $A^\nu$  is defined as  $A^\nu = \delta_0^\nu g A_a^0 \frac{\lambda_a}{2}$  with the gauge field  $A_a^\nu$ , the Gell-Mann matrix  $\lambda_a$  and the gauge coupling  $g$ . The matrix  $\vec{\tau}$  stands for the isospin matrix and  $G_s$  denotes the coupling constant of the scalar-type four-quark interaction. For simplicity, we neglect the vector-type four-quark interaction, since it does not change the conclusion of this paper qualitatively.

In the PNJL model, the gauge field  $A_\mu$  is treated as a homogeneous and static background field  $A_0$ , that is,  $A_\mu = \delta_{0\mu} A_0$ . In the Polyakov gauge, the Polyakov loop and its Hermitian conjugate,  $\Phi$  and  $\bar{\Phi}$ , are diagonal in color space:

$$\Phi = \frac{1}{3} \text{tr}_c(L), \quad \bar{\Phi} = \frac{1}{3} \text{tr}_c(\bar{L}) \quad (3)$$

with

$$L = e^{iA_4/T} = \text{diag}\left(e^{i\phi_a/T}, e^{i\phi_b/T}, e^{-i(\phi_a+\phi_b)/T}\right), \quad (4)$$

where  $\phi_a$  and  $\phi_b$  are classical variables and  $A_4 = iA_0$ .

We make the mean field approximation (MFA) to the quark-quark interactions in (2), as follows. In (2), the operator product  $\bar{q}q$  is first divided into  $\bar{q}q = \sigma + (\bar{q}q)'$  with the mean field

$\sigma \equiv \langle \bar{q}q \rangle$  and the fluctuation  $(\bar{q}q)'$ . Ignoring the higher-order terms of  $(\bar{q}q)'$  in the rewritten Lagrangian and resubstituting  $(\bar{q}q)' = \bar{q}q - \sigma$  into the approximated Lagrangian, one can obtain a linearized Lagrangian based on MFA,

$$\mathcal{L}_{\text{PNJL}}^{\text{MFA}} = \bar{q}(i\gamma_\nu \partial^\nu + i\gamma_0 A_4 - M)q - G_s \sigma^2 - \mathcal{U}(\Phi[A], \bar{\Phi}[A], T), \quad (5)$$

where  $M$  is the effective quark mass defined by  $M = m_0 - 2G_s \sigma$ . In (5), use has been made of  $\langle \bar{q}i\gamma_5\vec{\tau}q \rangle = 0$ , because the ground state is assumed to be invariant under the parity transformation. In the MFA Lagrangian  $\mathcal{L}_{\text{PNJL}}^{\text{MFA}}$ , quark fields interact only with the homogeneous and static back ground fields  $A_0$  and  $\sigma$ . Hence, we can easily make the path integral over the quark field to get the thermodynamic potential per unit volume,

$$\Omega_{\text{PNJL}} = -2N_f \int \frac{d^3p}{(2\pi)^3} \left[ 3E_p + \frac{1}{\beta} \ln [1 + 3(\Phi + \bar{\Phi}e^{-\beta(E_p-\mu)})e^{-\beta(E_p-\mu)} + e^{-3\beta(E_p-\mu)}] + \frac{1}{\beta} \ln [1 + 3(\bar{\Phi} + \Phi e^{-\beta(E_p+\mu)})e^{-\beta(E_p+\mu)} + e^{-3\beta(E_p+\mu)}] \right] + U_M + \mathcal{U}, \quad (6)$$

where  $\mu = \mu_R + i\mu_I = \mu_R + iT\theta$ ,  $E_p = \sqrt{\mathbf{p}^2 + M^2}$  and  $U_M = G_s \sigma^2$ .

The thermodynamic potential  $\Omega_{\text{PNJL}}$  is invariant under the extended  $\mathbb{Z}_3$  transformation [32],

$$e^{\pm i\theta} \rightarrow e^{\pm i\theta} e^{\pm i\frac{2\pi k}{3}}, \quad \Phi(\theta) \rightarrow \Phi(\theta) e^{-i\frac{2\pi k}{3}}, \\ \bar{\Phi}(\theta) \rightarrow \bar{\Phi}(\theta) e^{i\frac{2\pi k}{3}}. \quad (7)$$

This is easily understood by introducing the modified Polyakov loop,  $\Psi \equiv e^{i\theta}\Phi$  and  $\bar{\Psi} \equiv e^{-i\theta}\bar{\Phi}$ , invariant under the the extended  $\mathbb{Z}_3$  transformation (7), since  $\Omega_{\text{PNJL}}$  is described as a function of only the extended  $\mathbb{Z}_3$  invariant quantities,  $\Psi$ ,  $\bar{\Psi}$ ,  $\sigma$  and  $e^{3i\theta}$

$$\Omega_{\text{PNJL}} = -2N_f \int \frac{d^3p}{(2\pi)^3} \left[ 3E_p + \frac{1}{\beta} \ln [1 + 3\Psi e^{-\beta E_p} + 3\bar{\Psi}^* e^{-2\beta E_p} e^{i3\theta} + e^{-3\beta E_p} e^{i3\theta}] + \frac{1}{\beta} \ln [1 + 3\bar{\Psi}^* e^{-\beta E_p} + 3\Psi e^{-2\beta E_p} e^{-i3\theta} + e^{-3\beta E_p} e^{-i3\theta}] \right] + U_M + \mathcal{U}. \quad (8)$$

The physical quantities  $X = \sigma, \Psi$  and  $\bar{\Psi}$  are determined by the stationary conditions  $\partial\Omega_{\text{PNJL}}/\partial X = 0$ . These equations include the  $\theta$ -dependence only through the factor  $e^{3i\theta}$ , indicating that the  $X$  have the RW periodicity,  $X(\theta) = X(\theta + 2\pi k/3)$ . Inserting the solutions back to  $\Omega_{\text{PNJL}}$ , one can see that  $\Omega_{\text{PNJL}}$  also has the RW periodicity,  $\Omega_{\text{PNJL}}(\theta) = \Omega_{\text{PNJL}}(\theta + 2\pi k/3)$ ; see [32] for the details.

We take the three-dimensional momentum cutoff because this model is nonrenormalizable,

$$\int \frac{d^3p}{(2\pi)^3} \rightarrow \frac{1}{2\pi^2} \int_0^\Lambda dp p^2. \quad (9)$$

Hence, the present model has three parameters  $m_0$ ,  $\Lambda$  and  $G_s$ . We take  $\Lambda = 0.6315$  GeV and  $G_s = 5.498$  GeV $^{-2}$  so as to reproduce the pion decay constant  $f_\pi = 93.3$  MeV and the pion mass  $M_\pi = 138$  MeV at  $T = \mu = 0$ , when a realistic quark mass  $m_0 = 5.5$  MeV is taken [31, 35].

We use  $\mathcal{U}$  of Ref. [17] fitted to LQCD data in the pure gauge theory at finite  $T$  [36, 37]:

$$\frac{\mathcal{U}}{T^4} = -\frac{b_2(T)}{2}\bar{\Phi}\Phi - \frac{b_3}{6}(\bar{\Phi}^3 + \Phi^3) + \frac{b_4}{4}(\bar{\Phi}\Phi)^2, \quad (10)$$

$$b_2(T) = a_0 + a_1\left(\frac{T_0}{T}\right) + a_2\left(\frac{T_0}{T}\right)^2 + a_3\left(\frac{T_0}{T}\right)^3. \quad (11)$$

Following Ref. [32], we take  $T_0 = 190$  MeV so as to reproduce the pseudo-critical temperature  $T_c$  of the deconfinement phase transition at  $\mu = 0$  evaluated by LQCD; specifically,  $T_c$  is 170 MeV in the PNJL model, whereas it is  $173 \pm 8$  MeV in full LQCD calculations [38]. Thus, the present four parameters are determined from the pion mass and the pion decay constant at  $T = \mu = 0$  and LQCD data at  $T > 0$  and  $\mu = 0$ . However, if the vector-type four-quark interaction  $(\bar{q}\gamma_\mu q)^2$  is added to  $\mathcal{L}$ , the strength can not be determined at  $\mu = 0$ , since its mean field  $n = \langle \bar{q}\gamma_0 q \rangle$  is zero there. The strength will be determined by physical quantities at finite  $\theta$  such as meson masses, if they become available in the future.

### III. MESON MASS

In this section, we consider pion and sigma meson and derive equations for the meson masses, following Ref [21]. Correlators of current operators carry physical mesons with the quantum number. The pseudoscalar isovector current with the same quantum number as pion is

$$J_P^a(x) = \bar{q}(x)i\gamma_5\tau^a q(x) \quad (12)$$

and the scalar isoscalar current with the same quantum number as sigma meson is

$$J_S(x) = \bar{q}(x)q(x) - \langle \bar{q}(x)q(x) \rangle. \quad (13)$$

The Fourier transform of the mesonic correlation function  $\langle 0|T\left(J_\xi^a(x)J_\xi^{b\dagger}(0)\right)|0\rangle$  is defined as

$$\begin{aligned} C_{\xi\xi}^{ab}(q^2) &\equiv i \int d^4x e^{iq\cdot x} \langle 0|T\left(J_\xi^a(x)J_\xi^{b\dagger}(0)\right)|0\rangle \\ &= C_{\xi\xi}(q^2)\delta^{ab}, \end{aligned} \quad (14)$$

where  $\xi = P$  for pion and  $S$  for sigma meson and  $T$  stands for the time-ordered product. Using the random phase approximation (the ring approximation), one can obtain the Schwinger-Dyson equation for  $C_{\xi\xi}$  at  $T = \mu = 0$  where  $\Phi = \bar{\Phi} = 0$ ,

$$C_{\xi\xi}(q^2) = \Pi_{\xi\xi}(q^2) + 2G_s\Pi_{\xi\xi}(q^2)C_{\xi\xi} \quad (15)$$

with the one-loop polarization function

$$\Pi_{\xi\xi} \equiv (-i) \int \frac{d^4p}{(2\pi)^4} \text{Tr}(\Gamma_\xi iS(p+q)\Gamma_\xi iS(q)), \quad (16)$$

where  $S(q)$  is the quark propagator in the Hartree approximation and  $\Gamma_\xi = \Gamma_P^a = i\gamma_5\tau^a$  for pion and  $\Gamma_\xi = \Gamma_S = 1$  for sigma meson. In the random phase approximation, the solution to (15) is given as

$$C_{\xi\xi} = \frac{\Pi_{\xi\xi}(q^2)}{1 - 2G_s\Pi_{\xi\xi}(q^2)}. \quad (17)$$

Noting that meson mass  $M_\xi$  ( $\xi = \pi$  and  $\sigma$ ) is a pole mass of  $C_{\xi\xi}(q^2)$  and taking the rest frame  $q = (q_0, 0)$ , one can get an equation for  $M_\xi$  as

$$\left[1 - 2G_{\xi\xi}\Pi_{\xi\xi}(q_0)\right]_{q_0=M_\xi} = 0. \quad (18)$$

The explicit forms of  $\Pi_{PP}(q_0)$  and  $\Pi_{SS}(q_0)$  are given as

$$\begin{aligned} \Pi_{PP}(q_0) &= -i\text{Tr} \int \frac{d^4p}{(2\pi)^4} [i\gamma_5\vec{\tau}iS(p+q_0/2)i\gamma_5\vec{\tau}iS(p-q_0/2)] \\ &= 4i \text{tr}_c \int \frac{d^4p}{(2\pi)^4} \frac{(p+q_0/2)(p-q_0/2) - M^2}{[(p+q_0/2)^2 - M^2 + i\epsilon]} \\ &\quad \times \frac{1}{[(p-q_0/2)^2 - M^2 + i\epsilon]}, \end{aligned} \quad (19)$$

$$\begin{aligned} \Pi_{SS}(q_0) &= -i\text{Tr} \int \frac{d^4p}{(2\pi)^4} [iS(p+q_0/2)iS(p-q_0/2)] \\ &= 4i \text{tr}_c \int \frac{d^4p}{(2\pi)^4} \frac{(p+q_0/2)(p-q_0/2) + M^2}{[(p+q_0/2)^2 - M^2 + i\epsilon]} \\ &\quad \times \frac{1}{[(p-q_0/2)^2 + M^2 + i\epsilon]}, \end{aligned} \quad (20)$$

where  $\text{Tr}$  denotes  $\text{tr}_{\text{Dirac}} \otimes \text{tr}_{\text{Spin}} \otimes \text{tr}_c \otimes \text{tr}_{\text{Flavor}}$ .

When  $T$  and  $\mu$  are finite, the corresponding equations are obtained by the replacement

$$\begin{aligned} p_0 &\rightarrow i\omega_n + \mu + iA_4 = (2n+1)\pi T + \mu + iA_4, \\ \int \frac{d^4p}{(2\pi)^4} &\rightarrow iT \sum_n \int \frac{d^3p}{(2\pi)^3}. \end{aligned} \quad (21)$$

Also in this case, an equation for meson mass  $M_\xi$  is of the same form as (18), but the polarization functions are obtained in more complicated forms:

$$\Pi_{PP}(q_0) = -2N_f[2A(\mu) - q_0^2 B(q_0, \mu)] \quad (22)$$

for pion and

$$\Pi_{SS}(q_0) = -2N_f[2A(\mu) - (q_0^2 - 4M^2)B(q_0, \mu)], \quad (23)$$

for sigma meson. Here,  $A(\mu)$  and  $B(q_0, \mu)$  denote loop integrals [39] defined by

$$A(\mu) = \int \frac{d^3p}{(2\pi)^3} \frac{1 - f_{\text{PNJL}}(E_p - \mu) - f_{\text{PNJL}}(E_p + \mu)}{2E_p}, \quad (24)$$

$$B(q_0, \mu) = \int \frac{d^3p}{(2\pi)^3} \frac{1 - f_{\text{PNJL}}(E_p - \mu) - f_{\text{PNJL}}(E_p + \mu)}{E_p(q_0^2 - 4E_p)}, \quad (25)$$

where  $f_{\text{PNJL}}(E_p \pm \mu)$  is the modified Fermi-Dirac distribution function [21] defined by

$$f_{\text{PNJL}}(E_p - \mu) = \frac{(\Phi + 2\bar{\Phi}e^{-\beta(E_p - \mu)})e^{-\beta(E_p - \mu)} + e^{-3\beta(E_p - \mu)}}{1 + 3(\Phi + \bar{\Phi}e^{-\beta(E_p - \mu)})e^{-\beta(E_p - \mu)} + e^{-3\beta(E_p - \mu)}}. \quad (26)$$

The distribution function  $f_{\text{PNJL}}(E_p + \mu)$  is obtained by replacing  $-\mu \rightarrow +\mu$ ,  $\Phi \rightarrow \bar{\Phi}$  and  $\bar{\Phi} \rightarrow \Phi$ . In actual PNJL calculations, the imaginary part of meson mass  $M_\xi$  is assumed to be negligible in (18); this assumption is exactly satisfied when  $M_x$  is smaller than twice the dynamical quark mass,  $2M$ , and approximately satisfied for  $M_x$  slightly above  $2M$ .

In the case of  $\mu = i\mu_I = iT\theta$ , the corresponding distribution functions

$$f_{\text{PNJL}}(E_p - iT\theta) = \frac{\Psi + 2\bar{\Psi}e^{-\beta E_p}e^{3i\theta} + e^{-3\beta E_p}e^{3i\theta}}{1 + 3(\Psi + \bar{\Psi}e^{-\beta E_p}e^{3i\theta}) + e^{-3\beta E_p}e^{3i\theta}}, \quad (27)$$

depend only on the extended  $\mathbb{Z}_3$  invariant quantities,  $\Psi$ ,  $\bar{\Psi}$ ,  $\sigma$  and  $e^{3i\theta}$ . The distribution function  $f_{\text{PNJL}}(E_p - iT\theta)$  is obtained by replacing  $\theta \rightarrow -\theta$ ,  $\Psi \rightarrow \bar{\Psi}$  and  $\bar{\Psi} \rightarrow \Psi$ . Therefore, the distribution functions are also extended  $\mathbb{Z}_3$  invariant, and hence they have the RW periodicity. Furthermore, the polarization functions  $\Pi_{\xi\xi}$  depend on  $\theta$  only through the modified Fermi-Dirac distribution function  $f_{\text{PNJL}}(E_p \pm iT\theta)$ . Therefore, the meson masses have the RW periodicity.

#### IV. NUMERICAL RESULTS

First, we investigate the  $\mu$  dependence of pi and sigma meson masses,  $M_\pi$  and  $M_\sigma$ , in the  $\mu_R$  and  $\mu_I$  regions. It is found from (24) and (25) that  $M_\pi$  and  $M_\sigma$  are symmetric under the interchange  $\mu \leftrightarrow -\mu$ , indicating that they are functions of  $\mu^2$ . Figure 1 presents the  $\mu^2$  dependence of  $M_\sigma$  and  $M_\pi$  in the case of  $T = 160$  MeV that is near the pseudo-critical temperature  $T_c = 170$  MeV of the deconfinement phase transition at  $\mu = 0$ . They are smooth at  $\mu^2 = 0$ , as expected. This makes it possible the analytic continuation of meson masses,  $M_\pi(\mu)$  and  $M_\sigma(\mu)$ , from  $\mu = i\mu_I$  to  $\mu = \mu_R$ . This is important for LQCD simulation, although the PNJL calculation does not need the analytic continuation. In the right-half panel representing the  $\mu_R$  region,  $M_\pi$  and  $M_\sigma$  agree with each other when  $\mu^2 \gtrsim 0.1$  GeV<sup>2</sup>. This clearly exhibits that the restoration of chiral symmetry takes place at  $\mu^2 \gtrsim 0.1$  GeV<sup>2</sup> [21]. In the left-half panel representing the  $\mu_I$  region,  $M_\pi$  and  $M_\sigma$  look almost constant in this scale, but one can see oscillations of the masses on closer inspection shown by the inset and Fig. 2 that presents  $M_\pi$  and  $M_\sigma$  as a function of  $\theta$ .

In our previous paper [32], we showed that  $\theta$ -odd quantities with the RW periodicity such as  $d\Omega_{\text{PNJL}}/d\theta$  and the imaginary part of  $\Psi$  are discontinuous at  $\theta = \pi/3 \pmod{2\pi/3}$  and  $T \geq 190$  MeV. This first-order transition is called the RW phase transition. Meanwhile,  $\theta$ -even quantities with the RW periodicity such as  $\sigma$  and the real part of  $\Psi$  are discontinuous

in their derivative [32]. This indicates that the meson masses  $M_\xi$  have the same property as the chiral condensate. Actually, Fig. 2 shows that the  $M_\xi$  are  $\theta$ -even functions with the RW periodicity and then not smooth on the RW phase transition line.

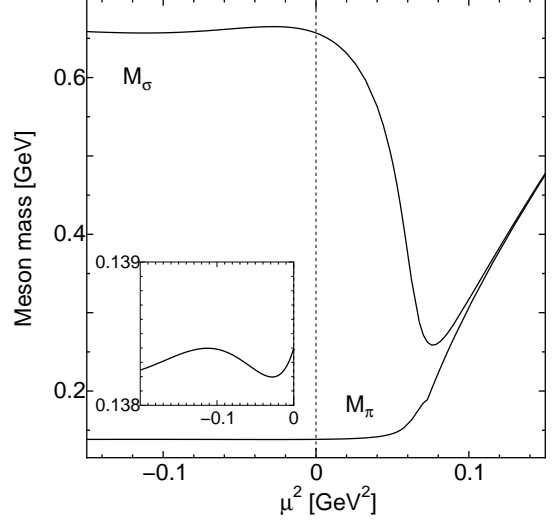


Fig. 1: The  $\mu^2$ -dependence of sigma and pi meson masses,  $M_\sigma$  and  $M_\pi$ , at  $T = 160$  MeV. The inset represents the pion mass near  $\mu = 0$ .

As an important property, the phase of oscillation is opposite to each other between  $M_\sigma$  and  $M_\pi$ . This can be understood from their slopes at  $\mu^2 = 0$ ;  $dM_\sigma/d\mu^2 < 0$  while  $dM_\pi/d\mu^2 > 0$  as shown in the inset of Fig. 1. These slopes reflect the chiral symmetry restoration appearing at  $\mu^2 > 0$ . Another point to be noted is the difference in their amplitudes; the amplitude of oscillation is relatively larger in  $M_\sigma$  whereas very small in  $M_\pi$ . This can be understood from (22) and (23); the latter has a term depending on the effective quark mass  $M$  and consequently reflects the chiral symmetry restoration directly, while the former does not.

The meson mass  $M_\xi(\theta)$  is a  $\theta$ -even function with the RW periodicity in the  $\mu_I$  region. This means that  $M_\xi(\theta)$  can be expanded in terms of  $\cos(3k\theta)$  with integer  $k$ :

$$M_\xi(\theta) = \sum_{k=0} a_k(T) \cos(3k\theta). \quad (28)$$

When  $T = 160$  MeV, the normalized coefficients  $a_k(T)/a_0(T)$  are about 0.1 % for  $k = 1$  and negligibly small for  $k \geq 2$ . The neglect of the normalized coefficients with  $k \geq 2$  is a good approximation at  $T$  near and below  $T_c$ . Particularly in the strong coupling limit of LQCD, the  $a_k$  with  $k \geq 2$  are known to be zero [40]. Hence,  $M_\xi(\theta)$  is approximated into

$$M_\xi^{\text{fit}} = A(T) \cos(3\theta) + C(T), \quad (29)$$

where  $A(T)$  and  $C(T)$  are determined from  $M_\xi$  at  $\theta = 0$  and  $\pi/3$  as

$$A(T) = [M_\xi(T, \theta = 0) - M_\xi(T, \theta = \pi/3)]/2, \quad (30)$$

$$C(T) = [M_\xi(T, \theta = 0) + M_\xi(T, \theta = \pi/3)]/2. \quad (31)$$

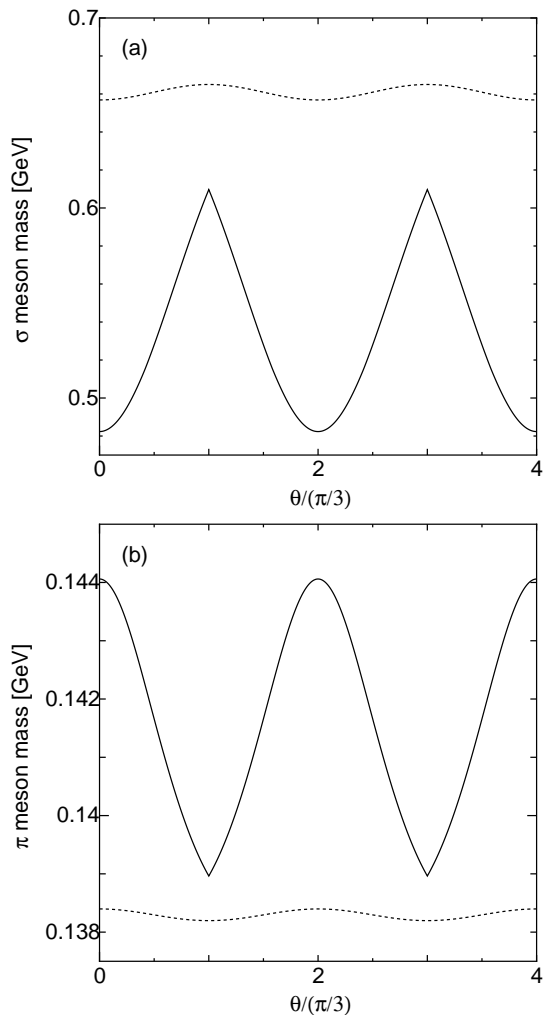


Fig. 2:  $\theta$  dependence of (a) sigma and (b) pi meson masses. Dotted curves denote the results of  $T = 160$  MeV and solid curves correspond to the results of  $T = 200$  MeV. Note that the scales of the vertical axes are different between panels (a) and (b).

Figure 3 shows  $A$  and  $C$  for the case of  $M_\pi$ . They smoothly increase with increase in  $T$  except a dip around  $T = 237$  MeV that comes from a threshold effect due to  $\pi \rightarrow$  quark + antiquark. The ratio  $A/C$  also becomes large as  $T$  increases. This means that the  $\theta$ -dependence of  $M_\pi$  becomes stronger as  $T$  increases. It is then preferable that LQCD simulations will be made at higher temperature near  $T_c$  except the dip temperature, in order to determine the parameters of the PNJL model more accurately. The  $\theta$ -dependence of meson masses at lower  $T$  can be extracted from LQCD data at higher  $T$  by using the PNJL model.

If  $A = 0$ ,  $M_\xi$  will have no  $\theta$  dependence, as shown by (29). The fact that  $A/C$  is small, then, indicates that the  $\theta$  dependence of  $M_\xi$  is rather weak. Figure 4 presents the  $T$ -dependence of pion mass at  $\theta = 0$  and  $\pi/6$ , where results of  $\theta = \pi/6$  ( $\theta = 0$ ) are represented by solid (dotted) curves. As expected, the overall behavior is almost the same between

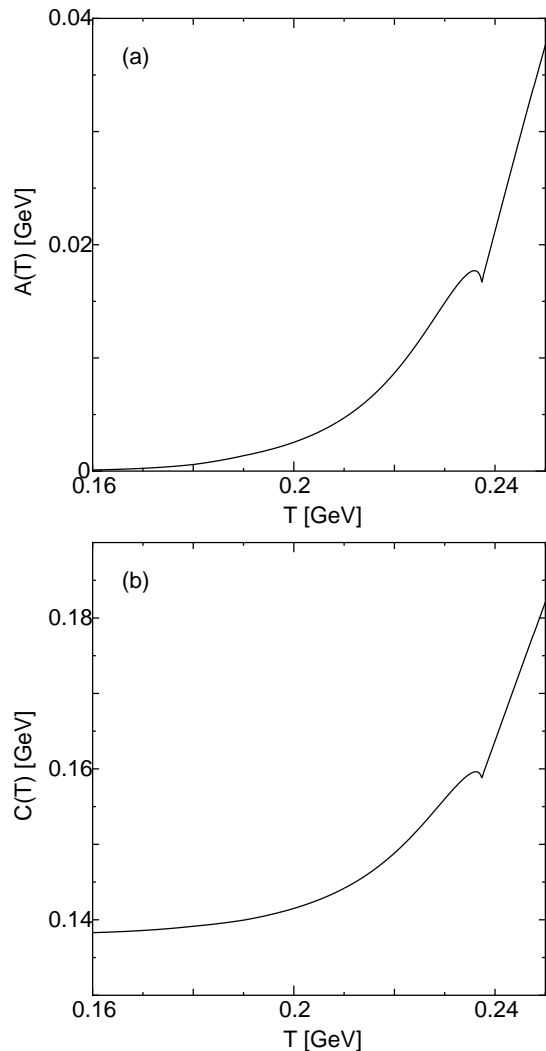


Fig. 3:  $T$ -dependence of  $A(T)$  and  $C(T)$  for the case of pion mass.

the two cases and the difference between the two is not large, although the crossing point where  $M_\pi = 2M$  is shifted to higher  $T$  as  $\theta$  increases.

The extrapolation of  $M_\xi$  from  $\mu^2 < 0$  to  $\mu^2 \geq 0$  was necessary for LQCD at least so far. Actually, LQCD data at  $\mu^2 < 0$  were extrapolated to the  $\mu^2 \geq 0$  region by assuming some fitting functions [4, 5, 6]. In the PNJL model, physical quantities are calculable directly in the  $\mu^2 \geq 0$  region, if the parameter set is determined from LQCD data in the  $\mu^2 \leq 0$  region. Here we assume the present PNJL result as a result of this  $\theta$ -matching approach and compare it with results of usual extrapolations in order to test the validity of the extrapolations. We consider two extrapolations. The first one is

$$M_\pi^{\text{fit}}(\mu/T) = A(T) \cosh(3\mu/T) + C(T). \quad (32)$$

When  $\mu = i\mu_I$ , Eq. (32) equals to Eq. (29). This form of  $M_\pi^{\text{fit}}$  has an exponential  $\mu$ -dependence at  $\mu = \mu_R$ . This extrapolation is then called the exponential extrapolation in this paper;

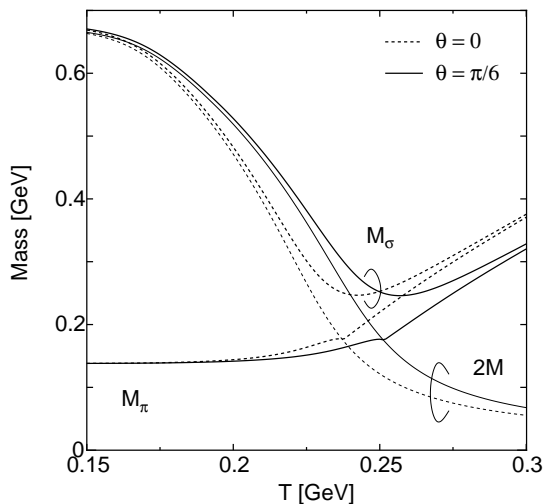


Fig. 4:  $T$ -dependence of sigma and pion masses at  $\theta = 0$  and  $\pi/6$ . Twice the constituent quark mass  $M$  is also shown.

a similar form is used in Ref. [5] for thermodynamical quantities rather than meson masses. The second is the polynomial extrapolation [4, 6] in which a polynomial of  $\mu^2$  is taken up to eighth order.

In Fig. 6,  $M_\pi$  calculated with the exponential and the polynomial extrapolation are compared with the result of the PNJL model. In the two simple extrapolations, their parameters are fitted to the PNJL result for  $\mu^2 \leq 0$  at  $T = 160$  MeV. At  $\mu^2 \leq 0$ ,  $M_\pi^{\text{fit}}$  agrees with  $M_\pi$  calculated with the PNJL model within thickness of curves. This means that the  $a_k$  for  $k \geq 2$  are tiny in the expansion (28). The two simple extrapolations give almost the same result for  $\mu^2 > 0$ . Thus, the polynomial extrapolation often used so far is essentially equal to the exponential one. The PNJL result and the results of the two extrapolations coincide accurately up to  $\mu_R/T \simeq 1$ .

Next, we discuss mathematically on the analytic continuation of  $M_\xi$  from  $\mu = i\mu_I$  to  $\mu = \mu_R + i\mu_I$ . First, we assume that LQCD gives  $M_\xi$  numerically in the  $\mu_I$  region. In order to make the analytic continuation, we need an analytic form of  $M_\xi$  that is valid in the  $\mu_I$  region. The Fourier expansion series (28) gives such an exact form of  $M_\xi$ , since  $M_\xi$  is a  $\theta$ -even function with the RW periodicity. As shown below,  $M_\xi$  has no  $\theta$  dependence in the low- $T$  limit and then all the  $a_k$  except  $a_0$  tend to zero in the limit. The partition function  $Z_{\text{GC}}(\theta)$  with a finite value of  $\theta$  is equivalent to  $Z_{\text{GC}}(0)$  with the boundary condition  $q(x, 1/T) = -\exp(i\theta)q(x, 0)$  for the quark field  $q$  [33]. In the low- $T$  limit where a period  $1/T$  of the imaginary time becomes infinite, the value of  $Z_{\text{GC}}(0)$  does not depend on how to take the boundary condition and then has no  $\theta$  dependence. The PNJL model can reproduce this property, as proven in Ref. [32].

As a result of the analytic continuation from  $\mu = i\mu_I$  to  $\mu = \mu_R + i\mu_I$ , the series becomes

$$M_\xi(\mu) = \sum_{k=0} a_k(T) \cosh(3k\mu/T). \quad (33)$$

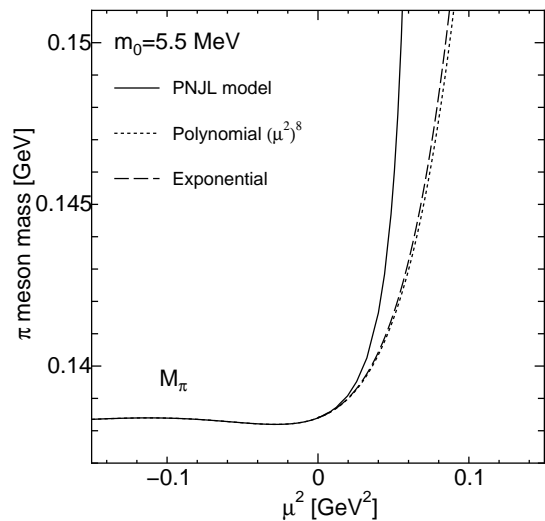


Fig. 5:  $\mu^2$ -dependence of  $M_\pi$  and  $M_\pi^{\text{fit}}$  at  $T=160$  MeV. The solid curve represents the PNJL result, the dotted curve does a fitted one by a polynomial up to  $(\mu^2)^8$  and the dashed curve does a fitted one by (29).

This is a natural extension of the exponential extrapolation (32). This form is valid, if the series converges. The condition for the convergence is

$$R \equiv \lim_{k \rightarrow \infty} \left| \frac{a_{k+1}(T) \cosh(3(k+1)\mu/T)}{a_k(T) \cosh(3k\mu/T)} \right| < 1. \quad (34)$$

In general,  $R$  depends on  $\mu$  and  $T$ . Now we consider the case of  $\mu = \mu_R$ . In the low- $T$  limit, all the  $a_k$  except  $a_0$  tend to zero, as mentioned above, while the factor  $\cosh(3(k+1)\mu_R/T)/\cosh(3k\mu_R/T)$  diverges for all  $k$ . Thus, there is a possibility that  $R$  is less than 1 even in the low- $T$  limit. However, it is impossible to evaluate the extremely small coefficients  $a_k$  ( $k \geq 1$ ) from LQCD data in the finite  $\theta$  region. Also for large  $T$  near  $T_c$ , the PNJL calculation shows that the coefficients  $a_k$  with  $k \geq 2$  are negligibly small. It is then difficult to evaluate the small coefficients from LQCD data with finite errors in the finite  $\theta$  region. Hence we propose to use the  $\theta$ -matching approach based on the PNJL model instead of the exponential and polynomial extrapolations and the analytic continuation (33).

Finally, we check an influence of the current quark mass  $m_0$  on the  $\mu$ -dependence of  $M_\pi$ , since large  $m_0$  is taken in LQCD simulations at finite  $\theta$ . The result adopting  $m_0 = 80$  MeV is shown in Fig. 6, for example. This figure indicates that, with heavy  $m_0$ , the sign of  $dM_\pi/d\mu^2$  at  $\mu^2 = 0$  becomes opposite to the case of light  $m_0$  shown in Fig. 1. This should be noticed.

## V. SUMMARY

We have analyzed, by using the PNJL model, the  $\mu$ -dependence of pi and sigma meson masses in both the  $\mu_R$

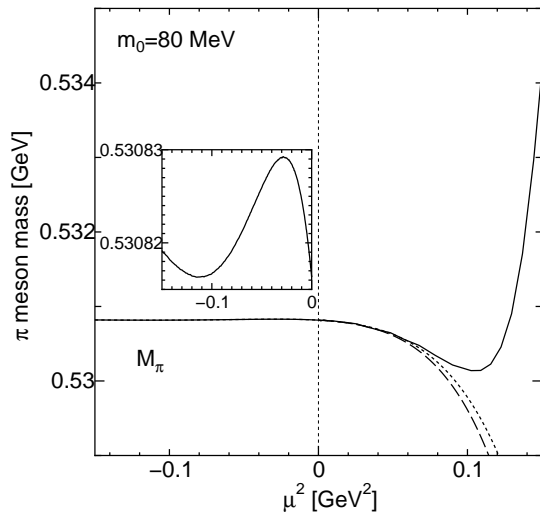


Fig. 6:  $\mu^2$ -dependence of pion mass at  $T = 160$  MeV in the case of  $m_0 = 80$  MeV. Definition of curves is the same as in Fig. ??.

and  $\mu_I$  regions. In the  $\mu_I$  region, the meson masses  $M_\xi(\theta)$  ( $\xi = \pi$  and  $\sigma$ ) are even functions of  $\theta$  with the RW periodicity:  $M_\xi(\theta) = M_\xi(-\theta) = M_\xi(\theta + 2k\pi/3)$ . This property is the same as that of the chiral condensate. The RW periodicity indicates that in general  $M_\xi(\theta)$  are oscillating with  $\theta$ . The amplitude of the oscillation becomes large as  $T$  increases. We then recommend that LQCD calculations be done at higher  $T$  near the pseudo-critical temperature  $T_c$  of the deconfinement phase transition at  $\mu = 0$ , in order to determine the parameters of the PNJL model more accurately. The  $\theta$ -dependence of meson masses at lower  $T$  can be extracted from the LQCD

data at higher  $T$  by using the PNJL model. As for pion mass  $M_\pi(\theta)$ , it should be noticed that the phase of the oscillation is rather sensitive to the value of the current quark mass  $m_0$ .

It is possible to do the PNJL calculation with a parameter set common between the  $\mu_R$  and  $\mu_I$  regions. Hence, we can argue that meson masses and other physical quantities in the  $\mu_R$  region can be extracted from LQCD data on meson mass at (1) finite  $T$  and zero  $\mu$  and (2) finite  $T$  and nonzero  $\mu_I$ , by using the PNJL calculation the parameters of which are fixed to the LQCD data. The present PNJL model has three parameters,  $m_0$ ,  $\Lambda$ ,  $G_s$ , in the quark sector and one parameter  $T_0$  in the gauge sector. As an extension of this minimal PNJL model, the vector-type four-quark interaction and/or the scalar-type eight-quark one are occasionally added to the present Lagrangian [32, 41]. All the parameters can be determined from LQCD data at the two cases; a trial is shown in Ref. [41]. The polynomial and exponential extrapolations used so far are accurate at  $\mu_R/T \lesssim 1$ . The  $\theta$ -matching approach based on the PNJL model is expected to be one of the most reliable methods to get physical quantities at finite  $\mu_R$ , if LQCD data on  $M_\xi(\theta)$  become available in the near future. We recommend that LQCD simulations be done systematically with the same lattice size between two cases of (1) finite  $T$  and zero  $\mu$  and (2) finite  $T$  and nonzero  $\mu_I$ .

#### Acknowledgments

H.K. thanks M. Imachi, H. Yoneyama and M. Tachibana for useful discussions. K.K. thanks T. Matsumoto for careful checks of numerical calculations. This work has been supported in part by the Grants-in-Aid for Scientific Research (18540280) of Education, Science, Sports, and Culture of Japan.

- 
- [1] J. B. Kogut, and D. K. Sinclair, Phys. Rev. D **77**, 114503 (2008).
  - [2] Z. Fodor, and S. D. Katz, Phys. Lett. B **534**, 87 (2002); J. High Energy Phys. **03**, 014 (2002).
  - [3] C. R. Allton, S. Ejiri, S. J. Hands, O. Kaczmarek, F. Karsch, E. Laermann, Ch. Schmidt, and L. Scorzato, Phys. Rev. D **66**, 074507 (2002); S. Ejiri, C. R. Allton, S. J. Hands, O. Kaczmarek, F. Karsch, E. Laermann, and Ch. Schmidt, Prog. Theor. Phys. Suppl. **153**, 118 (2004).
  - [4] P. de Forcrand and O. Philipsen, Nucl. Phys. **B642**, 290 (2002); P. de Forcrand and O. Philipsen, Nucl. Phys. **B673**, 170 (2003).
  - [5] M. D'Elia and M. P. Lombardo, Phys. Rev. D **70**, 074509 (2004).
  - [6] M. D'Elia and M. P. Lombardo, Phys. Rev. D **67**, 014505 (2003); M. P. Lombardo, PoSCPOD2006, 003 (2006).
  - [7] M. Asakawa and K. Yazaki, Nucl. Phys. **A504**, 668 (1989).
  - [8] J. Berges and K. Rajagopal, Nucl. Phys. **B538**, 215 (1999).
  - [9] O. Scavenius, Á. Mócsy, I. N. Mishustin, and D. H. Rischke, Phys. Rev. C **64**, 045202 (2001).
  - [10] H. Fujii, Phys. Rev. D **67**, 094018 (2003).
  - [11] M. Kitazawa, T. Koide, T. Kunihiro, and Y. Nemoto, Prog. Theor. Phys. **108**, 929 (2002).
  - [12] P. N. Meisinger, and M. C. Ogilvie, Phys. Lett. B **379**, 163 (1996).
  - [13] A. Dumitru, and R. D. Pisarski, Phys. Rev. D **66**, 096003 (2002); A. Dumitru, Y. Hatta, J. Lenaghan, K. Orginos, and R. D. Pisarski, Phys. Rev. D **70**, 034511 (2004); A. Dumitru, R. D. Pisarski, and D. Zschiesche, Phys. Rev. D **72**, 065008 (2005).
  - [14] K. Fukushima, Phys. Lett. B **591**, 277 (2004).
  - [15] S. K. Ghosh, T. K. Mukherjee, M. G. Mustafa, and R. Ray, Phys. Rev. D **73**, 114007 (2006).
  - [16] E. Megías, E. R. Arriola, and L. L. Salcedo, Phys. Rev. D **74**, 065005 (2006).
  - [17] C. Ratti, M. A. Thaler, and W. Weise, Phys. Rev. D **73**, 014019 (2006).
  - [18] M. Ciminale, R. Gatto, G. Nardulli, and M. Ruggieri, Phys. Lett. B **657**, 64 (2007); M. Ciminale, R. Gatto, N. D. Ippolito, G. Nardulli, and M. Ruggieri, Phys. Rev. D **77**, 054023 (2008).
  - [19] C. Ratti, S. Rößner, M. A. Thaler, and W. Weise, Eur. Phys. J. C **49**, 213 (2007).
  - [20] S. Rößner, C. Ratti, and W. Weise, Phys. Rev. D **75**, 034007 (2007).
  - [21] H. Hansen, W. M. Alberico, A. Beraudo, A. Molinari, M. Nardi, and C. Ratti, Phys. Rev. D **75**, 065004 (2007).
  - [22] C. Sasaki, B. Friman, and K. Redlich, Phys. Rev. D **75**, 074013 (2007).

- [23] B. -J. Schaefer, J. M. Pawłowski, and J. Wambach, Phys. Rev. D **76**, 074023 (2007).
- [24] P. Costa, C. A. de Sousa, M. C. Ruivo, and H. Hansen, arXiv:hep-ph/0801.3616; P. Costa, M. C. Ruivo, C. A. de Sousa, H. Hansen, and W. M. Alberico, arXiv:hep-ph/0807.2134.
- [25] K. Kashiwa, H. Kouno, M. Matsuzaki, and M. Yahiro, Phys. Lett. B **662**, 26 (2008).
- [26] H. Abuki, M. Ciminale, R. Gatto, G. Nardulli, and M. Ruggieri, Phys. Rev. D **77**, 074018 (2008); H. Abuki, M. Ciminale, R. Gatto, N. D. Ippolito, G. Nardulli, and M. Ruggieri, Phys. Rev. D **78**, 014002 (2008); H. Abuki, R. Anglani, R. Gatto, G. Nardulli, and M. Ruggieri, Phys. Rev. D **78**, 034034 (2008); H. Abuki, M. Ciminale, R. Gatto, and M. Ruggieri, Phys. Rev. D **79**, 034021 (2009).
- [27] W. J. Fu, Z. Zhang, and Y. X. Liu, Phys. Rev. D **77**, 014006 (2008).
- [28] K. Fukushima, Phys. Rev. D **77**, 114028 (2008); Phys. Rev. D **78**, 114019 (2008).
- [29] T. Hell, S. Rößner, M. Cristoforetti, and W. Weise, Phys. Rev. D **79**, 014022 (2009).
- [30] H. M. Tsai, and B. Müller, arXiv:hep-ph/0811.2216.
- [31] K. Kashiwa, H. Kouno, T. Sakaguchi, M. Matsuzaki, and M. Yahiro, Phys. Lett. B **647**, 446 (2007).
- [32] Y. Sakai, K. Kashiwa, H. Kouno, and M. Yahiro, Phys. Rev. D **77**, 051901(R) (2008); Phys. Rev. D **78**, 036001 (2008); Y. Sakai, K. Kashiwa, H. Kouno, M. Matsuzaki, and M. Yahiro, Phys. Rev. D **78**, 076007 (2008).
- [33] A. Roberge and N. Weiss, Nucl. Phys. **B275**, 734 (1986).
- [34] L. K. Wu, X. Q. Luo, and H. S. Chen, Phys. Rev. D **76**, 034505 (2007).
- [35] K. Kashiwa, M. Matsuzaki, H. Kouno, and M. Yahiro, Phys. Lett. B **657**, 143 (2007).
- [36] G. Boyd, J. Engels, F. Karsch, E. Laermann, C. Legeland, M. Lütgemeier, and B. Petersson, Nucl. Phys. **B469**, 419 (1996).
- [37] O. Kaczmarek, F. Karsch, P. Petreczky, and F. Zantow, Phys. Lett. B **543**, 41 (2002).
- [38] F. Karsch, E. Laermann, and A. Peikert, Nucl. Phys. B **605**, 579 (2001).
- [39] See, e.g., A. L. Fetter, and J. D. Walecka, *Quantum Theory of Many-Particle System* (McGraw-Hill, New York, 1971).
- [40] N. Kawamoto, K. Miura, A. Ohnishi, and T. Ohnuma, Phys. Rev. D **75**, 014502 (2007).
- [41] Y. Sakai, K. Kashiwa, H. Kouno, M. Matsuzaki, and M. Yahiro, arXiv:hep-ph/0902.0487 [Phys. Rev. D (to be published)].